Scientific
Research
Publishing

Geochemical Study of Almoqlaq Intrusive Body in North of Asadabad in Hamedan Province, Iran

Ahmad Farnin

Islamic Azad University, North Tehran Branch, Tehran, Iran
Email: Ahmad.farnin@hotmail.com

Abstract

The study area is located in the west of Iran and in the north of Asadabad. This is the range between Eastern lengths of 00', 48° to 15', 48°, and northern latitudes of 45', 34° to 00', 35°. This range is limited from north to the asphalt road of Hamadan Qorveh, Sanandaj, and from the East and Southeast, to Asadabad of Kermanshah-Hamedan road, and from the West to Chahardoli plain and from the south to the plains and the town of Asadabad. According to the geological map of the study area, intrusive outcropping of diorite-gabbro of Almoqlaq, and quartz syenite is at Almoqlaq mountains. Intrusive rocks of the region, based on the total Alkali oxide, against silica rocks of study area fall within the quartz monzonite, gabbro, granodiorite, granite, and syenite between quartz and alkali granite. And granite in the study area (due to aluminum saturation index), is in the range of metaluminous, and metaluminous to peraluminous. Based on normalized spider diagram with the upper crust, the typical study area belongs to this model, and most of the elements are placed near or on standard line of 1.

Keywords

Almoqlaq, Geochemistry, Intrusion, Alkali Granite, Metaluminous, Quartz Monzonite and Spider Diagram

1. Introduction

The study area is located in the west of Iran and in the north of Asadabad. This is the range between Eastern lengths of 00', 48° to 15', 48°, and northern latitudes of 45', 34° to 00', 35° (**Figure 1**). This range is limited from north to the asphalt road of Hamadan Qorveh, Sanandaj, and from the East and Southeast, to Asadabad of Kermanshah-Hamedan road, and from the West to Chahardoli plain and from the south to the plains and the town of
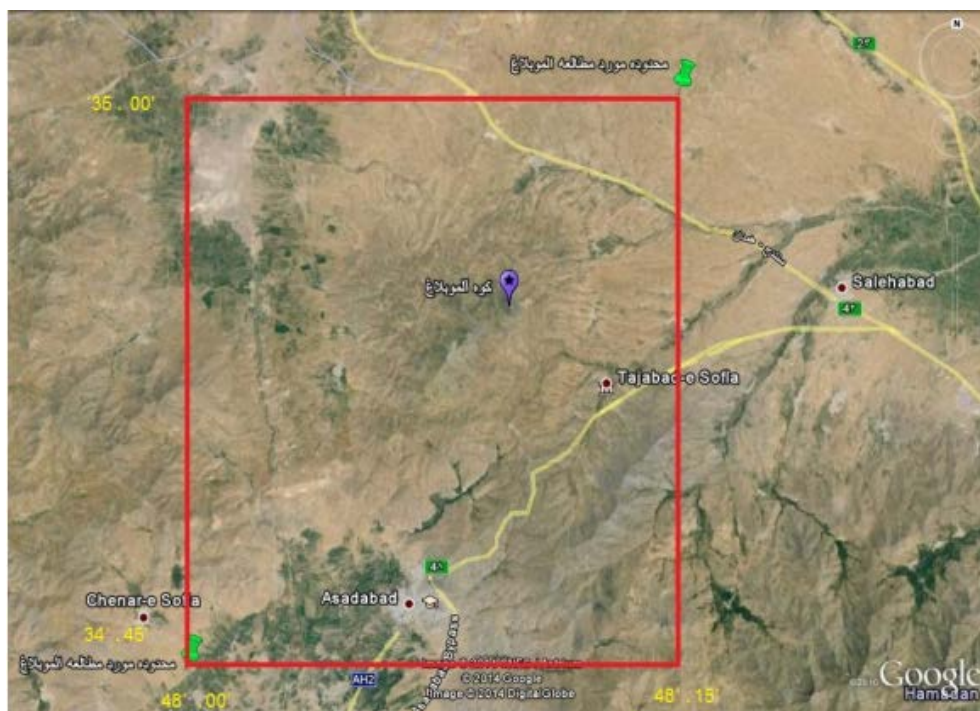
Figure 1. Satellite image of the study area (Source: Google Earth).

Asadabad.

In the north region, there are located Qeshlaq and Pahnebar and Hamekasi; and in the east it is limited to the villages of Ali Baba, Akhtehchi, Lower hand Tajiabad and DEHNO; and from the southeast it is limited to, Rasulabad village; from the west it is limited to the villages of Qarakand, Poshtdarband, Gholdareh, Pirmalu, Charuq; and from the south it is limited to villages of Tarkhinabad and the town of Asadabad (**Figure 2**).

2. Access to the Area

From Hamedan, this area is accessible by two paved roads. One by Hamedan-Asadabad road, in which, the study area is located in its West, and from Hamadan to the highest point of the road in Asadabad Gorge which is about 35 km away, and from there, via dirt road which was constructed by Department of Telecommunications, and then, by the ways paved for native access, access into the mountains of Almuglaq. Other road is from Hamadan to Sanandaj, from asphalt way to Hamekasi village, with a length of 25 km, and from there, to the village of Baba Ali, and lump iron ore. Also, by dirt-gravel roads, from Asadabad or from Hamekasi village, everyone can access to the plain of Chardoli and to Qarakand village, and then, by a narrow dirt road again to foothills of Almoqlaq (**Figure 2**).

Almoqlaq peak height is 2993 meters above sea level. Irregularities in the area are in the connection with lithological characteristics and tectonic phenomena, and from the perspective of the formation geomorphological Almoqlaq cone of High Mountain located in the proximity of Mount Alvand, its slope is moderate, and overall appearance is affected by the intrusion of Almoqlaq and evokes a dome-shaped bulge in the mind. Almoqlaq area, from the perspective of structural geology of Iran, is located in Sanandaj-Sirjan and has general characteristics of this zone.

3. Intrusive Bodies of Study Area

3.1. Almoqlaq Masses of Diorite-Gabbro

This mass is exposed at three points, but from the perspective of development, is much smaller than the mass of Alvand gabbro. Among these deposits, there are a number of dikes or Apophyses with microdioritic-dolerite combinations, which have genetic ties with the masses of diorite-gabbro of Almoqlaq. Stones related to the mass
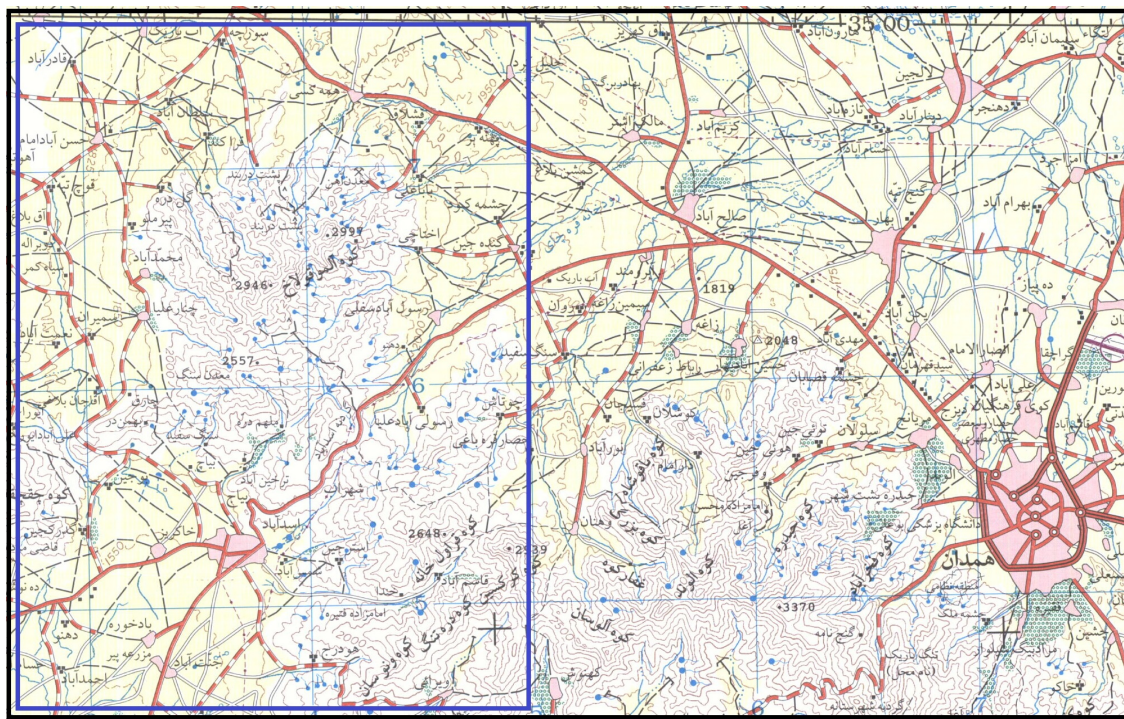
Figure 2. Map of access roads to the study area (topographic map 1:250,000 Hamadan, Armed Forces Geographical Organization, 2001; (Source: Google Earth).

are more likely from gray to light gray with green and sometimes dark spots.

3.2. Mass of Quartz Syenite in the Mountains of Almoqlaq

In Almoqlaq Mountains, there are many outcrops of quartz syenite rocks which are a combination of different cognitive stone, inclusind quartz syenite, granodiorite and quartz micro Monsosyenite. These rocks have gentle topography and for the most part, they are covered by debris. The results can be found in the following **Tables 1-3** and figures.

4. Observations and Results

In the diagram [1], it is used of alkali oxides ($Na_2O + K_2O$) in the silica of SiO_2 (**Figure 3**). As we can see in the diagram, ten samples were used namely, four samples in quartz monzonite border, one sample in monzonite and a sample in monzonite quartz border a sample is located on the border of quartz monzonite and granite, two located within granite, a sample is located in granite and granodiorite border and a sample located within the gabbro.

Delarosh *et al*. classification (1980) is based on cationic core elements ratios, and expressed as mg cation. In this category, the results are plotted on a graph of two variables of XY and using graphical parameters of R1, R2. In this diagram, R1 is placed in the X-axis, and R2 is located Y-axis. The cation graph defined by R2, R1, which is = 4 Si-11 (Na + K) − 2 (Fe + Ti) R1 and R2 = 6Ca + 2Mg + Al. Based on the chart below four samples of rocks studied area, ranging from quartz monzonite a sample of gabbro, a sample is within the granodiorite, three are in the range of granite, and an example is in the range between quartz alkali syenite and granite (**Figure 4**).

Change plot of K_2O versus SiO_2 are presented by changes in weight percentage, the two oxide K_2O and SiO_2, and it has been shown, 4 magmatic series tholeiitic, calc-alkaline, calc-alkaline which are rich in potassium and Shoshsonitic. According to this chart, two samples of rocks are located in tholeites range, two are in the range of calc-alkaline series, six samples are located in the series of calc-alkaline and rich in potassium (**Figure 5**).

In the classification of rocks on chart, (PQ chart Debon & Le Fort) was used by parameters P = K − (Na + Ca) and Q = Si/3 − (K + Na + 2Ca/3). With regard to this chart of the rocks in studied area, there are placed a sample

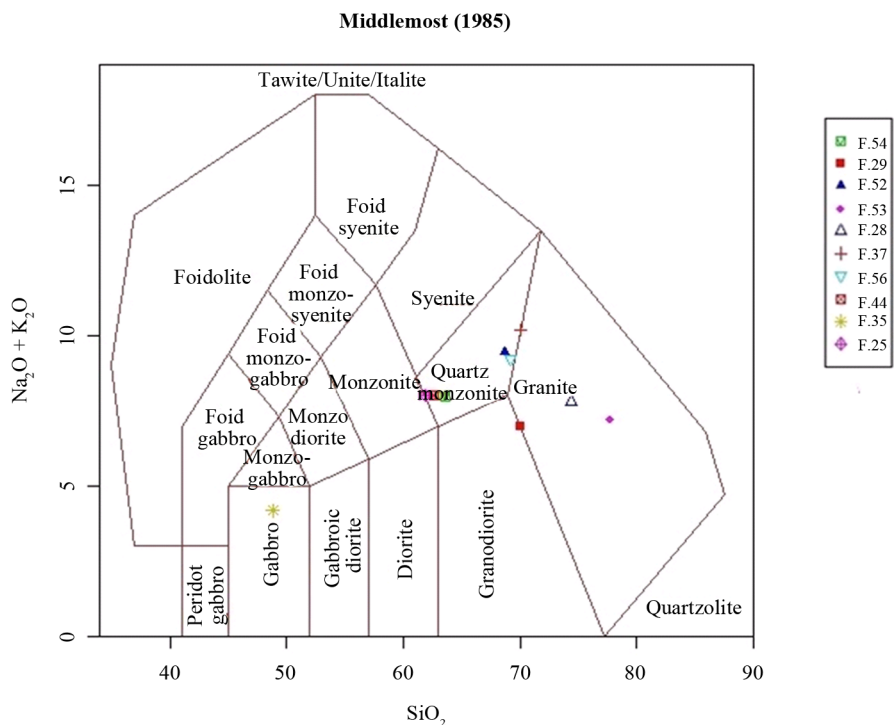**Figure 3.** Total alkali oxide (Na$_2$O + K$_2$O), against silica (SiO$_2$) [1].
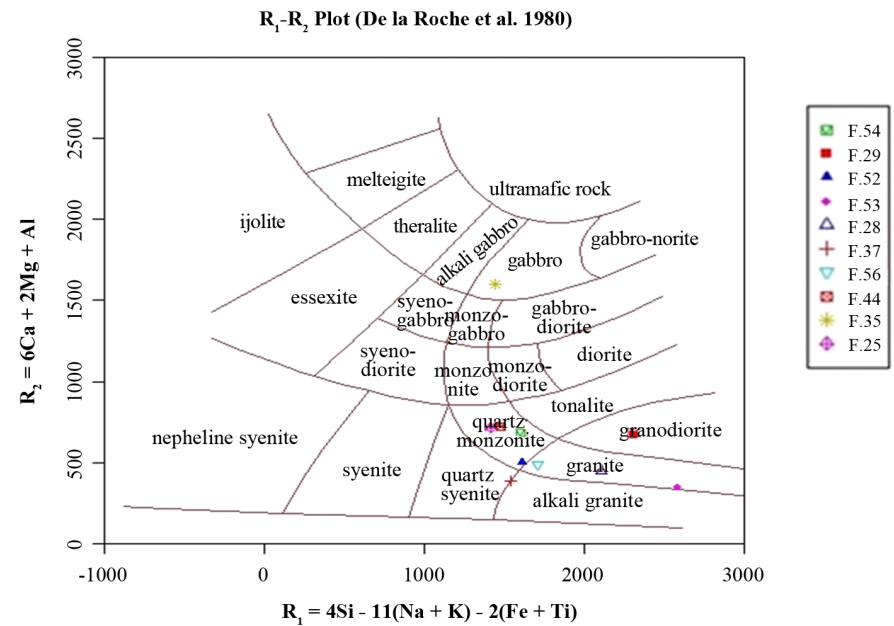

Figure 4. Classification charts of Delarosh *et al*., 1980 [2].

of gabbro, two of tonalite, a sample of granodiorite sample, two samples of quartz monzonite, three samples of quartz, and one sample are located out of the defined range (**Figure 6**).

Wilson classification [2]: the base of this classification is the chart of total alkali versus silica (TAS) of Cox *et al*. (1979), for volcanic rocks which by Wilson [2] has been extended to intrusive rocks. Existing the separating line in alkaline range from sub-alkali, is a feature of this chart. In this diagram (**Figure 7**), of the rocks of studied area, four samples are located in the range of intermediate, five samples are located in granite range (acidic), and
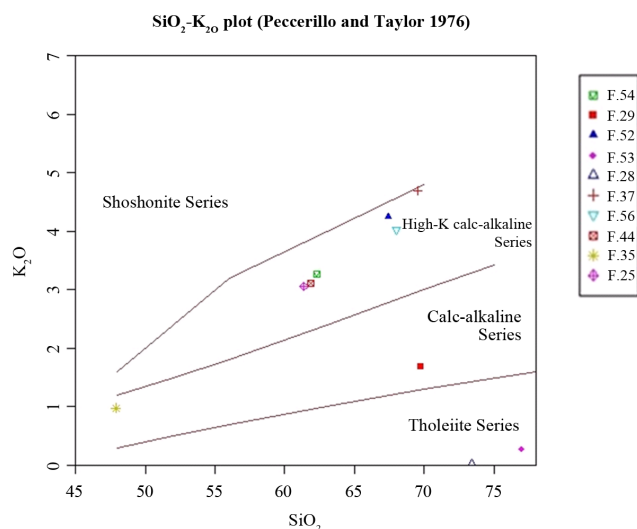
SiO₂-K₂O plot (Peccerillo and Taylor 1976)

Figure 5. Change plot of K₂O versus SiO₂ (Peccerillo and Taylor, 1976) [2].
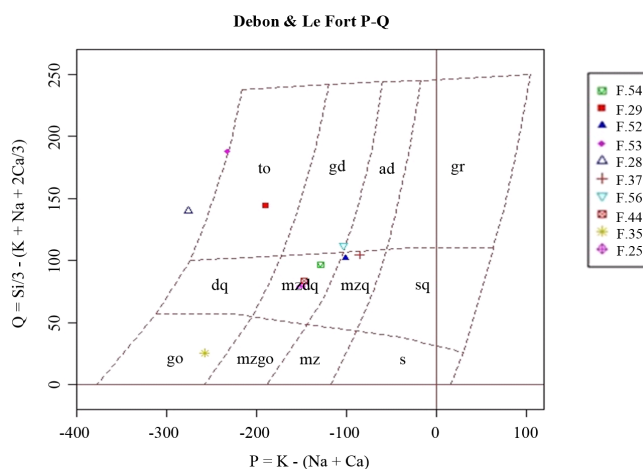
Debon & Le Fort P-Q

Figure 6. Classification of rocks based on the diagram (Debon & Le Fort PQ) [2].

Table 1. Chemical analysis of the main elements of the study area (author finding).

S.N.	F.52	F.29	F.53	F.25	F.54	F.28	F.56	F.35	F.44	F.37
Formula	(%)	(%)	(%)	(%)	(%)	(%)	(%)	(%)	(%)	(%)
SiO_2	67.41	69.76	76.96	61.39	62.32	73.42	68.03	47.89	61.85	69.52
Al_2O_3	15.34	16.21	12.73	16.15	15.96	13.69	15.24	14.53	16.11	15.84
Fe_2O_3	3.34	2.41	0.92	7.56	6.42	1.53	3.23	14.86	6.82	2.43
CaO	1.63	3.11	0.89	3.26	2.89	1.59	1.45	9.98	3.21	0.55
Na_2O	5.03	5.26	6.89	4.88	4.52	7.69	5.04	3.12	4.82	5.42
K_2O	4.25	1.69	0.27	3.06	3.26	0.02	4.02	0.98	3.11	4.69
MgO	0.48	0.44	0.15	0.96	1.18	0.27	0.69	4.96	1.29	0.32
TiO_2	0.561	0.542	0.191	1.334	0.968	0.493	0.451	1.536	1.201	0.352
MnO	0.048	0.021	0.005	0.123	0.115	0.016	0.067	0.146	0.147	0.007
P_2O_5	0.076	0.083	0.028	0.421	0.271	0.044	0.076	0.088	0.198	0.061
S	0.008	0.006	0.008	0.006	0.005	0.008	0.009	0.012	0.007	0.006
L.O.I	1.63	0.24	0.59	0.56	1.79	0.93	1.32	1.54	1.08	0.55

Table 2. Normative composition in the samples of study area (author finding).

Sample	F.52	F.29	F.53	F.25	F.54	F.28	F.56	F.35	F.44	F.37
Q	18.079	25.26	34.062	14.129	16.365	25.97	19.407	3.116	13.991	18.561
C	0	0.272	0	0	0.39	0	0.143	0	0	0.993
Or	25.116	9.987	1.596	18.084	19.266	0.118	23.757	5.791	18.379	27.716
Ab	42.562	44.509	58.301	41.293	38.247	65.071	42.647	26.401	40.786	45.863
An	6.725	14.887	3.01	13.124	12.567	2.777	6.697	22.747	13.136	2.33
Di	0	0	0.434	0	0	1.451	0	16.627	0	0
Wo	0	0	0	0	0	0.531	0	0	0	0
Hy	1.196	1.096	0.172	2.391	2.939	0	1.719	4.646	3.213	0.797
Il	0.084	0.031	0	0.249	0.234	0.015	0.122	0.284	0.298	0.001
Hm	3.34	2.41	0.92	7.56	6.42	1.53	3.23	14.86	6.82	2.43
Tn	0.609	0	0.469	0.211	0	1.19	0	3.404	1.054	0
Ru	0.269	0.526	0	1.118	0.845	0	0.387	0	0.615	0.352
Ap	0.18	0.197	0.066	0.997	0.642	0.104	0.18	0.208	0.469	0.144
Pr	0.015	0.011	0.008	0.011	0.009	0.015	0.017	0.022	0.013	0.011
Sum	98.176	0.011	99.039	99.166	97.924	98.772	98.306	98.106	98.774	99.198

Table 3. The results of chemical analysis for trace elements, in the samples of the study area (in ppm) (author finding).

| Field num.	F.52	F.29	F.53	F.25	F.54	F.28	F.56	F.35	F.44	F.37
Cl	274	98	87	214	2215	54	324	4924	4028	136
Ba	542	368	280	660	565	380	512	334	680	343
Sr	172	480	133	293	165	105	134	227	169	27
Cu	13	21	24	25	20	17	20	31	23	41
Zn	58	27	18	89	88	27	53	66	85	31
Pb	8	7	16	5	14	6	9	8	18	19
Ni	38	37	40	40	36	43	31	63	34	39
Cr	8	9	11	9	5	7	5	31	7	5
V	50	63	25	104	115	57	52	325	122	42
Ce	85	49	51	22	43	59	49	35	89	49
La	28	22	28	8	21	30	22	14	32	19
W	8	5	4	8	14	6	6	5	2	2
Zr	460	565	344	347	395	430	430	86	328	496
Y	73	61	58	72	71	131	68	22	60	79
Rb	117	43	23	76	103	16	112	38	107	131
Co	8	5	11	8	12	9	11	9	12	8
As	2	11	21	5	4	42	5	5	7	19
U	6	2	1	2	8	2	2	1	2	1
Th	11	8	15	8	14	11	9	4	6	15
Mo	1	2	2	1	1	2	4	2	6	5
Ga	22	27	18	19	20	30	20	13	17	23
Nb	1	2	4	2	1	5	2	1	1	2
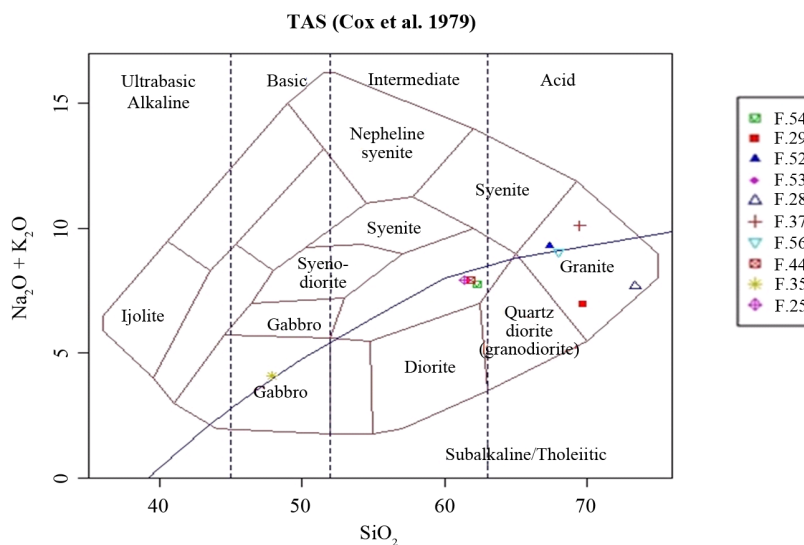
Figure 7. Geochemical classification of intrusive rocks using total figure of Alkali against silica (Cox *et al*., 1979) [2].

a sample is gabbro rocks and is located in basic range.

Classification of rocks based on Debon & Le Fort AB chart: This graph covers A = Al − (K + Na + 2Ca) and B = Fe + Mg + Ti parameters which is indicative of two ranges of Peraluminous and metaluminous. According to below diagram, three of the rocks are located in the study area of metaluminous, and contain biotite ± amphibole ± pyroxene Clino, four rock samples from the study area are located in the meta area, and the are composed of biotite, amphibole ± pyroxene, two are located on the border of Peraluminous and metaalumina (3 and 4) and the range includes biotite, amphibole, pyroxene and biotite ± a little bit of amphibole. One of the rocks range. one of the rocks of the study area is in the region of Peraluminous, and is located on the border of 2 and 3, which includes biotite ± a small amount of amphibole, muscovite and biotite. See **Figure 8**.

Classification of rocks based on (Alkali-Lime): In this graph which is introduced in the name of MALI, parameters of $(Na_2O + K_2O)$, in front of SiO_2 (**Figure 9**) are used. In this diagram, nine samples are in the range of calcite and a sample is placed in the alkaline range.

Todays, the saturation of aluminum has been accepted as an important factor in determining the origin of granitoid magma and is of particular importance. Based on this index, peraluminous granites are divided into 4 categories of metaluminous, Peralkaline and sub-alumina [3].

PerAlumina $Al_2O_3 > (Na_2O + K_2O + CaO)$

Metaluminous $(Na_2O + K_2O + CaO) > Al_2O_3 > (Na_2O + K_2O)$

Saab alumina $Al_2O_3 = (Na_2O + K_2O)$

Peralkaline $Al_2O_3 < (Na_2O + K_2O)$

Aluminium saturation index is defined by the following relationship:

Al/NK = $Al_2O_3/(Na_2O + K_2O)$

Al/CNK = $Al_2O_3/(Na_2O + K_2O + CaO)$

Based on the chart [3], seven samples are in the range of meta-alumina and two samples are on the border of meta-alumina to per-alumina, a sample located within Peraluminous (**Figure 10**).

Normalized graph of the area under study, with normal Mvrbhay, Sun & MacDonough 1989 [4]: According to this model, elements LILE) Rb, K (Ba, and light rare earths (LREE) (Ce, La), compared to the elements (Nb, Ti) HFS, enriched show, and in our model, most chemicals, placed on top of the standard line 1, the MORB. In this pattern, anomalies Pb observed. Based on these charts, examples area of study, depletion of elements P, Ti, and enriched Pb, and almost all elements, are higher than the standard line 1, the MORB, that this issue shows a lack of independence of the mantle source depleted (MORB) (**Figure 11**).

To evaluate changes in productive magma toward original one, as well as their origin and genetic relationship, the spider diagrams was used. According to this model, nearly all elements show enrichment, such as Th, U, Rb, with the exception of potassium, compared to primitive mantle. Enrichment of samples in the range of LILE,
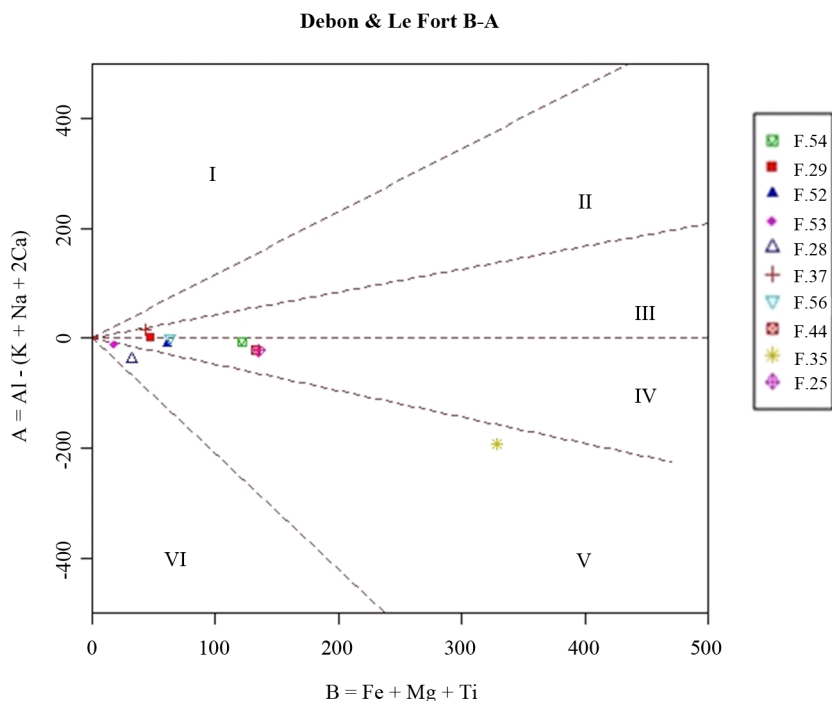
Debon & Le Fort B-A

Figure 8. Classification of rocks, according to the chart A (B) Debon & Le Fort [3].
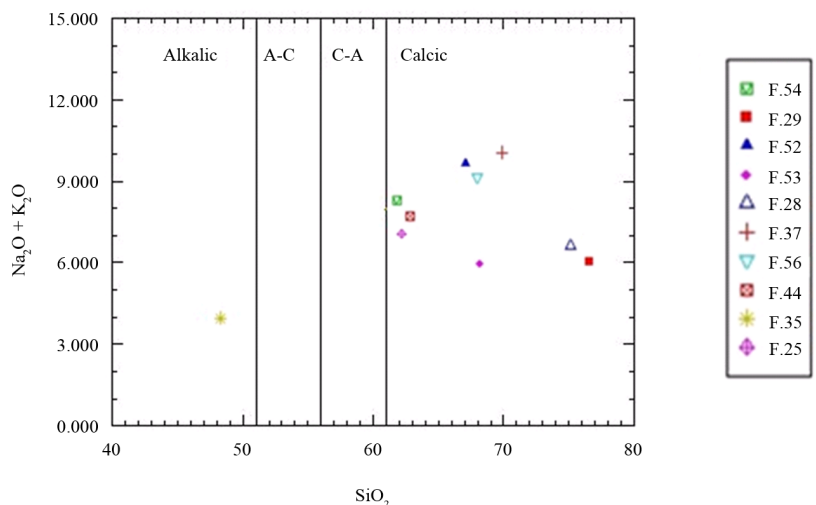

Figure 9. Classification based on Alkali-Lime (Peacock, 1931) Aluminium saturation index [3].

could be the result of magma fractionation and crustal contamination. Elements of Zr, Th, Y, have a positive anomaly, and these elements can indicate infection with the upper crust (**Figure 12**).

According to this model, the Nb element has negative anomaly, and to the upper crust, suggesting the depletion. Elements of Y, Zr are also central to the case, which has enriched and the positive anomalies of these elements may indicate infection with the upper crust. Most elements are near or on the standard line 1, the Upper crust (**Figure 13**).

5. Conclusions

According to petrographic studies, most igneous rocks of the study area, such as: Quartz syenite, which is a
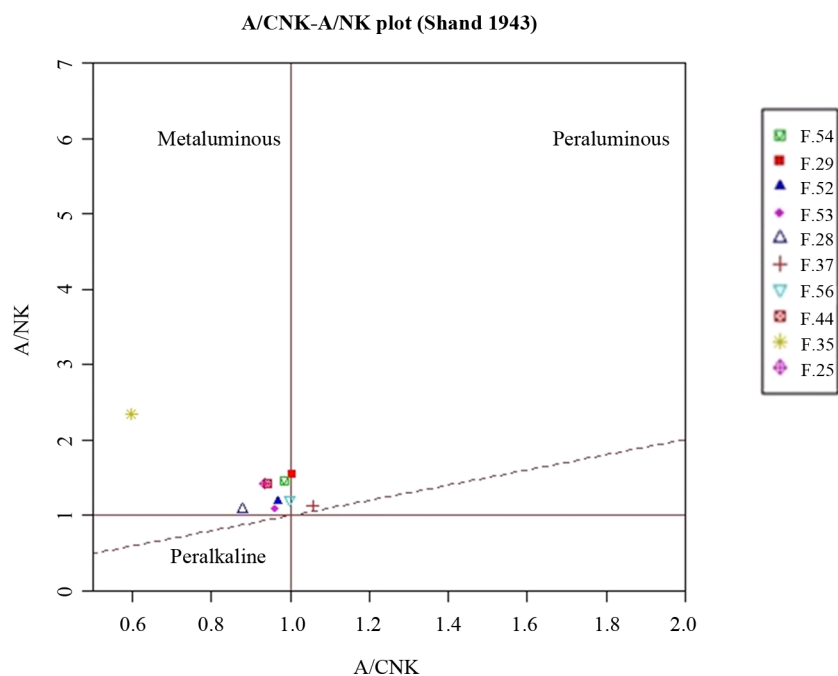
A/CNK-A/NK plot (Shand 1943)

Figure 10. The chart of A/NK against A/CNK to distinguish peraluminous, metaluminous and Peralkaline magmas [3].
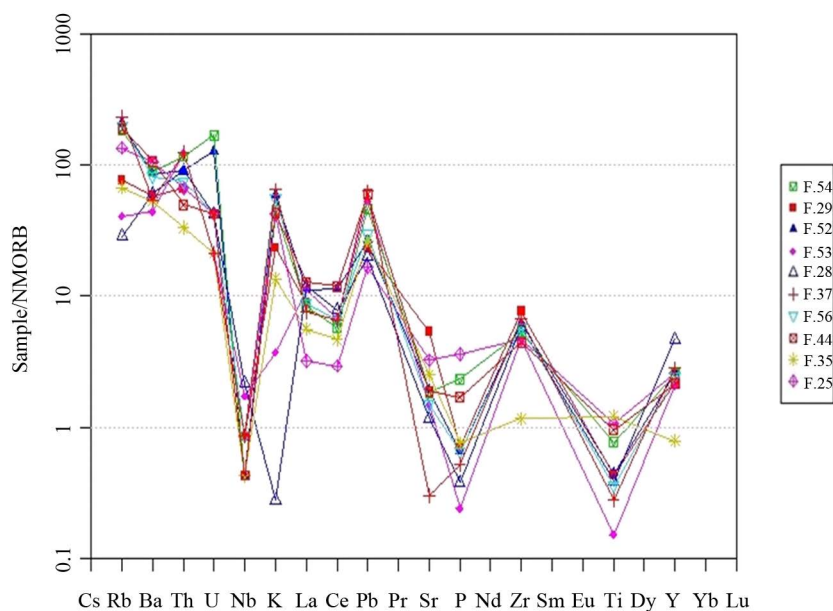

Figure 11. The normalized spider diagrams, from the study area samples with normal diagonals [4].

medium-grained texture and porphyric. Syenite and quartz syenite and plutonic rocks form the bulk of the region. Quartz hornblende syenite is a medium-grained texture, and little alteration in them. The stone, after the quartz syenite, forms the largest rocks in the study area. Alkali granite studied, mostly middle-crystal, is a Porphyric tissue, the tissue indicating shallow magma crystallization, and is often helocorate, or Lococrate. Other gems of the study area, syenite, are without quartz or quartz-poor, and pure tissue. Alkaline quartz syenite, this stone is structured grain. Monzonite, monzonite of the area is gray, and has an average grain texture. Hornblende diorite,
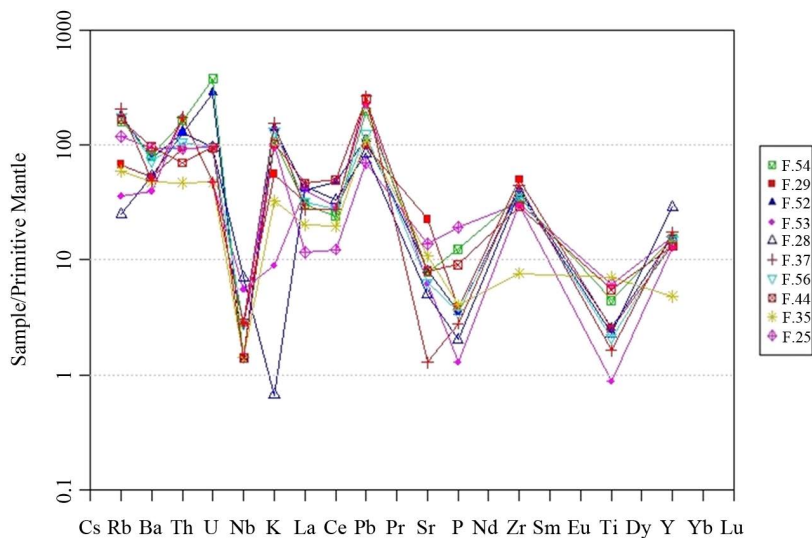
Figure 12. Charts the norm sample of the study area, with primitive mantle (MacDonough & Sun, 1989) [4].
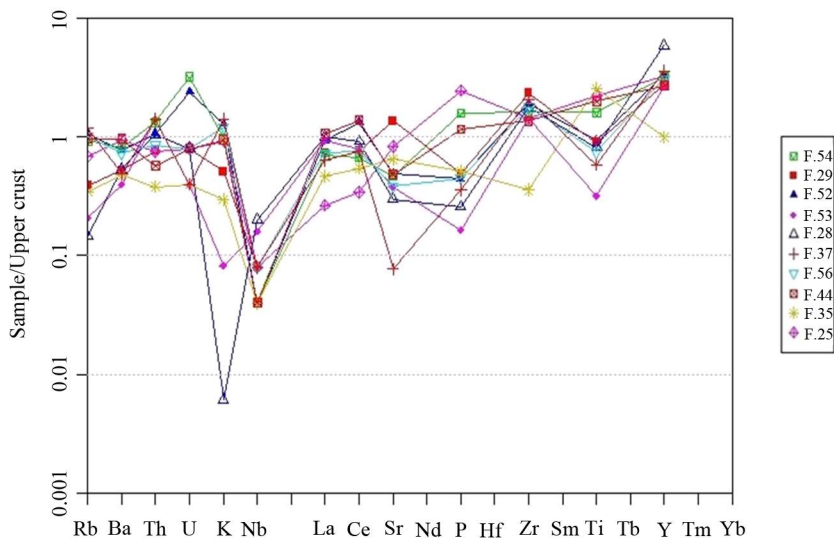

Figure 13. Normalized charts, samples of the study area, with the upper crust [5].

medium-grained texture, and rich hornblende and plagioclase, and the sample-and-white are gray.

These rocks are the main minerals including quartz, feldspar, plagioclase, hornblende, and minor minerals, not including Apec, and sphene, and biotite, and secondary minerals, chlorite and sericite are included. According to the graph, normalized samples studied area, with the upper crust, rocks of the study area belong to this pattern, and most elements are near or on line 1 standard.

Acknowledgements

References

[1]   Middlemost, E.A.K. (1985) Magmas and Magmatic Rocks. An Introduction to Igneous Petrology. Longman Group, UK, 73-87.

[2]   Wilson, R. (1990) Igneous Petrogenesis. Unwin Hyman Ltd., 466 p.

[3]   Shand, S.J. (1943) Coronas and Coronites. Bull. Geol. Soci. America, No. 56, 247-266.

[4]   Sun, S. and McDonough, W.F. (1989) Chemical and Isotopic Systematic of Oceanic Basalts: Implications for Mantle Composition and Processes. Geological Special Publication No. 42, 313-345.

[5]   Taylor, R.P. and Mclennan, S.M. (1985) The Continental Crust, Its Composition and Evolution. Black Wall, Oxford, 312 p.